Brillouin-scattering study of the liquid-glass transition in $CaKNO_3$: Mode-coupling analysis

N. J. Tao,* G. Li, and H. Z. Cummins
Department of Physics, City College of the City University of New York, New York, New York 10031
(Received 13 June 1991)

Polarized and depolarized Brillouin scattering from 0.4 $Ca(NO_3)_2$-0.6KNO_3 was investigated in the temperature range of 320 to 640 K using a six-pass Sandercock tandem Fabry-Perot interferometer. The polarized spectra were analyzed with a simplified version of mode-coupling theory, in which the small-q density fluctuation modes probed by light scattering couple only to pairs of modes at q_0 corresponding to the first peak in the structure factor $S(q)$. The density correlation function $\phi(q_0,t)$ determined by neutron spin-echo experiments by Mezei *et al.* was used as input in the analysis, producing excellent fits to the experimental data. The depolarized spectra were analyzed with a phenomenological viscoelastic model including NO_3^- orientational relaxation.

I. INTRODUCTION

The liquid-glass transition has been studied for many years, but a complete theory of this phenomenon has yet to be found.[1-3] Recently, renewed interest in this problem[4] has been stimulated by the mode-coupling theory (MCT), which predicts an ergodic-to-nonergodic transition with increasing undercooling of a liquid.[5-7] The MCT transition, which in the simple version of the theory is predicted to occur at a temperature T_c somewhat above the experimental glass transition temperature T_g, is a result of nonlinear interactions between density fluctuation modes leading to an eventual dynamical instability and structural arrest. The simple MCT, which does not include activated hopping processes, does not correctly predict behavior of real materials very close to T_g.[8] (The predictions of the more sophisticated version of the theory, which includes activated processes,[9] have not yet been determined.) However, for temperatures greater than $\sim 1.3T_g$, it predicts temperature dependences for various thermodynamic properties and transport coefficients which are in good agreement with many observations.[8,10-14] Several experiments have been carried out in recent years to test the predictions of MCT, including the predicted scaling laws for structural relaxation dynamics.

One of the central predictions of MCT is a scaling law for the α-relaxation process whose relaxation time τ diverges at a temperature T_c. According to this scaling law (or time-temperature superposition principle) the temperature dependence of structural dynamics in the supercooled liquid should only depend on temperature through the time scale $\tau(T)$ so that data acquired at different temperatures can be superimposed on a single master plot. This prediction is consistent with the frequently used approximation of a stretched-exponential time decay function $e^{-(t/\tau)^\beta}$ in which β is a temperature-independent constant. The scaling law is asymptotically valid for $T \to T_c^+$, with additional small T dependence possible far from T_c.

In another recent approach to the glass transition, Campbell *et al.*[15] have suggested that structural dynamics are associated with diffusion in the accessible volume of configuration space. Far above the glass transition, the accessible volume for n particles is a compact $3n$-dimensional hypercube and diffusional relaxation behaves as $e^{-t/\tau}$. As the temperature decreases, the accessible volume becomes successively more ramified, eventually evolving into a single percolation cluster and then fragmenting in the nonergodic phase into mutually inaccessible ramified clusters. As T approaches the percolation threshold (which may correspond to the glass transition), β should decrease, since diffusion at the percolation threshold behaves as $e^{-(t/\tau)^\beta}$ with $\beta \approx \frac{1}{3}$. This approach therefore predicts a strongly temperature dependent β, in disagreement with MCT.

Analysis of the temperature dependence of β therefore constitutes a critical test of the MCT. However, as Fuchs, Götze, and Latz[16] have recently pointed out, determination of β from the analysis of Brillouin scattering and ultrasonic data is frequently ambiguous. The measured value of β can, for example, depend on the time scale of the experimental technique. We will return to this question in the discussion and conclusions section.

Brillouin scattering has been widely applied to the study of the liquid-glass transition. In most cases, the analysis has been limited to the temperature dependence of the Brillouin shifts and linewidths interpreted by comparison with phenomenological viscoelastic theories. Recently several Brillouin scattering experiments have been reported in which the full spectrum was analyzed by fitting to a theoretical prediction for $I(\omega)$, thus providing a much more thorough test of the viscoelastic theory. These include a study of $ZnCl_2$ by Soltwisch, Sukmanowski, and Quitmann,[17] of propylene carbonate by Börjessen, Elmroth, and Torell,[18] and of LiCl-H_2O by Tao, Li, and Cummins.[19]

In our LiCl-H_2O paper,[19] we suggested that a simplified version of the MCT approach could be used to analyze the Brillouin scattering data. We carried out an analysis based on the Percus-Yevick equation, which produced qualitatively reasonable results but could not pro-

vide quantitative fits to the experimental data. The limited success of this analysis was most likely due either to the use of a one-component theory to describe an electrolyte or to the simple hard-sphere approximation underlying the Percus-Yevick equation.

In this communication, we report a new Brillouin scattering study of the glass forming mixed salt system $0.4Ca(NO_3)_2$-$0.6KNO_3$ (hereafter CKN; $T_g \sim 333$ K, $T_M = 438$ K). In our simplified MCT analysis we utilized the recent neutron-spin echo data of Mezei, Knaak, and Farago[10] rather than a model calculation for the density correlation function $\phi(q_0,t)$. The MCT analysis produced excellent agreement with our data, showing that in the limited range of relaxation times probed by Brillouin scattering ($10^{-11} < \tau < 10^{-8}$ sec) the simplified version of MCT works very well.

CKN is in many ways ideally suited to studies of the liquid-glass transition and has been the subject of many previous investigations. (We will present a brief review of previous work in Sec. VI.) It is easy to prepare, forms a colorless transparent glass, and has a convenient glass temperature. It lies close to the "fragile liquid" limit in Angell's classification scheme, demonstrating the absence of network structure.[8,20] The molten salt contains three ionic species; two of these, K^+ and Ca^{2+} are simple argonlike ions. But the third, NO_3^-, is optically anisotropic so that its orientational dynamics complicate the interpretation of the Brillouin spectra, particularly the depolarized spectra, a point we will discuss in detail in Sec. V.

II. THEORY

A. Simple fluids

In a simple structureless fluid, the linearized hydrodynamic equations predict five modes for each (small) wave vector q: two relaxing transverse velocity (or viscous shear) modes, a narrow quasielastic thermal diffusion mode, and two approximately Lorentzian longitudinal acoustic modes centered at $\omega_0 = C_0 q$, where C_0 is the adiabatic sound velocity ($C_0 = \sqrt{M/\rho}$, where M is the adiabatic compressional modulus and ρ is the density) with half width $\approx \frac{1}{2}[(\frac{4}{3}\eta_s + \eta_B)/\rho + (\Lambda/\rho)(1/C_v - 1/C_p)]$, where η_s and η_B are the shear and bulk viscosities, Λ is the thermal conductivity, and C_v and C_p are the specific heat at constant volume and pressure, respectively.[21]

In a Brillouin scattering experiment, the scattered spectrum $I_q(\omega)$ (with ω measured relative to the incident laser frequency) is proportional to the spectrum of the density fluctuations $(\rho_q^2)_\omega$. Since in simple fluids transverse velocity does not couple to the density, the viscous shear modes do not appear in the spectrum. The remaining three modes, which do couple to the density, produce the familiar triplet observed in Brillouin scattering experiments. The thermal diffusion mode occurs at frequencies well below the lower resolution limit (~ 0.1 GHz) normally accessible to Brillouin scattering and is therefore not resolved, although it can be studied by other techniques such as correlation spectroscopy,[22,23] forced Rayleigh scattering,[24] or the closely related impulsive stimulated Brillouin scattering.[25] Consequently, only the sound waves contribute to the Brillouin spectrum.

If we also ignore the contribution of thermal diffusion to the acoustic mode damping, the equation of motion for ρ_q appropriate for Brillouin scattering is

$$\ddot{\rho}_q + \left[\frac{M}{\rho} q^2\right] \rho_q + \left[\frac{\eta_L}{\rho} q^2\right] \dot{\rho}_q = 0 \tag{1}$$

or

$$\ddot{\rho}_q + \omega_0^2 \rho_q + \Gamma_0 \dot{\rho}_q = 0 \tag{2}$$

where $\eta_L = \frac{4}{3}\eta_s + \eta_B$ is the longitudinal viscosity.

The spectrum $I_q(\omega)$ can be found from Eq. (2) either by evaluating the density correlation function $F(q,t) = \langle \rho_q(0)\rho_q(t) \rangle = S(q)\phi_q(t)$ [the Fourier transform of $F(q,t)$ is the dynamic structure factor $S(q,\omega)$], or from the fluctuation-dissipation theorem

$$I_q(\omega) = \frac{I_0}{\omega} \operatorname{Im}\chi(\omega) , \tag{3}$$

where $\chi(\omega)$ is the complex frequency-dependent susceptibility.

Equations (1) and (3) yield, for the Brillouin spectrum

$$I(q,\omega) = \frac{I_0}{\omega} \operatorname{Im}\left[-\omega^2 + \frac{M}{\rho} q^2 - i\omega \frac{\eta_L}{\rho} q^2\right]^{-1}$$

$$= \frac{I_0}{\omega} \frac{\omega \eta_L q^2/\rho}{(\omega^2 - Mq^2/\rho)^2 + (\omega \eta_L q^2/\rho)^2} \tag{4}$$

or, with the abbreviation of Eq. (2),

$$I(q,\omega) = \frac{I_0}{\omega} \operatorname{Im}(-\omega^2 + \omega_0^2 - i\omega\Gamma_0)^{-1} . \tag{5}$$

B. Viscoelastic theories

As a fluid is cooled below its (crystal) melting temperature T_M, its viscosity increases rapidly and the thermodynamic properties of the undercooled melt become frequency dependent, signaling the increasingly long relaxation times associated with the evolving structural order. The structural relaxation processes can be incorporated phenomenologically into the hydrodynamic equations in several equivalent ways.[26]

The compressional modulus M in Eqs. (1) and (4) can be generalized to a frequency-dependent form $M(\omega) = M'(\omega) - iM''(\omega)$ by introducing a stress memory function $\phi_M(t)$ so that Eq. (4) becomes

$$I_q(\omega) = \frac{I_0}{\omega} \frac{[M''(\omega) + \omega\eta_L] q^2/\rho}{[\omega^2 - M'(\omega)q^2/\rho]^2 + [(M'' + \omega\eta_L)q^2/\rho]^2} . \tag{6}$$

(Note that if the viscous damping contribution is combined with the imaginary part of the compressional modulus $[M''(\omega) + \omega\eta_L \rightarrow M''(\omega)]$, then Eq. (6) is identical to the equation used by Fuchs, Götze, and Latz[16] in their reanalysis of ultrasonic and Brillouin scattering studies of CKN.) Rather than generalizing M, the longi-

tudinal viscosity η_L can be generalized to $\eta_L(\omega)$ by introducing a viscosity memory function $\phi_\eta(t)$. In the simplest single-relaxation-time approximation (Maxwell viscoelasticity), $\phi_\eta(t)=\eta_0\delta(t)+\eta_R e^{-t/\tau}$ and

$$\eta_L(\omega)=\eta_0+\frac{\eta_R}{1+i\omega\tau} , \tag{7}$$

where η_0 is the frequency-independent component of $\eta_L(\omega)$. Alternatively, the introduction of frequency-dependent transport or response coefficients can be avoided by introducing another phenomenological degree (or degrees) of freedom, which represents the "local structural order," and coupling it bilinearly to the density.

These approaches all lead to results that are formally equivalent, and which can all be represented by

$$I_q(\omega)=\frac{I_0}{\omega}\,\mathrm{Im}[\omega_0^2-\omega^2-i\omega\Gamma(\omega)]^{-1} =\frac{I_0}{\omega}\frac{\omega\Gamma'}{[\omega^2-(\omega_0^2+\omega\Gamma'')^2]^2+(\omega\Gamma')^2} , \tag{8}$$

where

$$\Gamma(\omega)=\Gamma'+i\Gamma''=\Gamma_0+\Delta^2\int_0^\infty e^{i\omega t}\phi_\Gamma(t)dt \tag{9}$$

is a generalized damping or friction function. In Eq. (9), $\phi_\Gamma(t)$ is the memory function for the damping.

In the single relaxation-time approximation, $\phi_\Gamma(t)=e^{-t/\tau}$, Eq. (8) reduces to

$$I_q(\omega)=\frac{I_0}{\omega}\,\mathrm{Im}\left[\omega_0^2-\omega^2-i\omega\left[\Gamma_0+\frac{\Delta^2\tau}{1-i\omega\tau}\right]\right]^{-1} . \tag{10}$$

Equation (10), which we used[27] in analyzing our LiCl-H_2O Brillouin data,[19] was also widely used in the 1970's to analyze the central-peak spectra observed in neutron or light scattering from crystals near structural phase transitions.[28]

Equation (8) can be easily generalized to more complicated memory functions such as the stretched-exponential (Kohlrausch) function,[29]

$$\phi_\Gamma(t)=e^{-(t/\tau)^\beta} , \tag{11}$$

or the closely related Cole-Davidson function for $\Gamma(\omega)$:[30]

$$\Gamma(\omega)=\Gamma_0+\Delta^2\left[\frac{1}{1-i\omega\tau}\right]^{\beta_{CD}} . \tag{12}$$

In their Brillouin scattering study of propylene carbonate, Börjesson, Elmroth, and Torell[18] used a theoretical formulation equivalent to Eqs. (8) and (12) and found that $\beta_{CD}\sim 0.4$, nearly independent of temperature, corresponding to β [in Eq. (11)] ~ 0.5.

We also note that Eq. (10) can be used to describe the collective excitations at q values beyond the range of validity of continuum hydrodynamics.[31] The approach of molecular hydrodynamics shows that this result still holds, but at large q values ω_0 is not proportional to the adiabatic sound speed C_0. Rather, $\omega_0(q)=(qv_0)^2/S(q)$, where v_0 is a thermal velocity.

C. Mode-coupling theory

The mode-coupling approach to the glass transition as proposed by Bengtzelius, Götze, and Sjolander in 1984,[5] begins with the expression for the complex reduced dynamic structure factor $\tilde{R}(q,\omega)=\tilde{S}(q,\omega)/S(q)$ [where $\tilde{S}(q,\omega)$ is the Fourier transform of the density correlation function $F(q,t)$]

$$\tilde{R}(q,\omega)=\frac{i}{\omega-\omega_0^2/[\omega+i\tilde{\Gamma}(q,\omega)]} . \tag{13}$$

[Note that the real part of $\tilde{R}(q,\omega)$ in Eq. (13), which is proportional to the scattered spectrum $I_q(\omega)$, reduces to Eq. (10) apart from a constant of proportionality.] The generalized damping function $\tilde{\Gamma}(q,\omega)=\Gamma'(\omega)+i\Gamma''(\omega)$ is then separated into two parts:

$$\tilde{\Gamma}(q,\omega)=\Gamma_0+\tilde{\Gamma}_{MC}(q,\omega) , \tag{14}$$

where the "background damping" term Γ_0, which is proportional to q^2, represents all high-frequency (nonrelaxing) processes. The mode-coupling term $\tilde{\Gamma}_{MC}(q,\omega)$ includes the damping processes resulting from nonlinear interactions between density modes. Its Fourier transform, $\Gamma(q,t)$, is given in leading order (three-mode interactions only) by

$$\Gamma(q,t)=(2\pi)^{-3}\int d^3\mathbf{q}'V(\mathbf{q},\mathbf{q}')\phi(\mathbf{q}',t)\phi(|\mathbf{q}-\mathbf{q}'|,t) , \tag{15}$$

where the vertex (or coupling) constant $V(\mathbf{q},\mathbf{q}')$ is given approximately by

$$V(\mathbf{q},\mathbf{q}')=\frac{nk_BT}{m}(\hat{\mathbf{q}}\cdot\hat{\mathbf{q}}')C(\hat{\mathbf{q}}')[(\hat{\mathbf{q}}\cdot\hat{\mathbf{q}}')C(\mathbf{q}')+\hat{\mathbf{q}}\cdot(\mathbf{q}-\mathbf{q}')C(\mathbf{q}-\mathbf{q}')]S(q')S(|\mathbf{q}-\mathbf{q}'|) . \tag{16}$$

In Eq. (16), $C(q)=[S(q)-1]/[nS(q)]$ and n is the number density. Thus, if $S(q)$ is known for all q as a function of T and n, $\tilde{S}(q,\omega)$ can be determined self-consistently using Eqs. (13)–(16).

It has been argued that the most important contribution to $\Gamma(q,t)$ comes from coupling to pairs of modes with $q\sim q_0$, where q_0 is the position of the first peak of $S(q)$.[5,32] If, as originally proposed by Bengtzelius, Götze, and Sjolander,[5] one simplifies Eq. (15) by including only modes with $q=q_0$ in the integral, then

$$\Gamma(q,t)=V_0\phi^2(q_0,t) , \tag{17}$$

where

$$V_0 = q^2[A^2\omega_0^2(q_0)/4\pi^2 n]S(q_0)[S(q_0)-1] , \quad (18)$$

and A is the area under the first peak of $S(q)$, above a baseline of 1.

In our previous Brillouin scattering study of aqueous LiCl solutions,[19] we used the Percus-Yevick equation to compute V_0 and $S(q_0)$ in Eq. (18). We then solved Eqs. (13), (14), and (17) self-consistently with $q = q_0$ to obtain $\phi(q_0,t)$, which was used to predict $\tilde{R}(q,\omega)$ for the small-q mode probed by Brillouin scattering.

In the present study, we were able to avoid this hard-sphere approximation completely, since Mezei, Knaak, and Farago[10] have measured $\phi(q_0,t)$, for CKN in neutron spin echo experiments. We were therefore able to use their data in Eq. (17), and then evalute $\tilde{R}(q,\omega)$ in Eq. (13) directly, treating V_0 and ω_0 as adjustable parameters.

We note that the simplified mode coupling result given by Eqs. (13), (14), and (17) is formally equivalent to the phenomenological result of Eqs. (8) and (9), with Δ^2 and $\phi_\Gamma(t)$ in Eq. (9) replaced by V_0 and $\phi^2(q_0,t)$ in Eq. (17). In fact, since the neutron data of Mezei, Knaak, and Farago are well described by the stretched exponential function $\phi(q_0,t) = ae^{-(t/\tau)^\beta}$, the mode coupling result is actually identical to the viscoelastic results of Eqs. (8) and (9) with $\phi_\Gamma(t) = a^2 e^{-2(t/\tau)^\beta}$. The essential difference is that τ and β, rather than being treated as phenomenological free parameters of the viscoelastic memory function, are physical microscopic coefficients in MCT, which can be determined experimentally by neutron scattering. Operationally, the number of free parameters is therefore reduced by two.

III. EXPERIMENTS AND RESULTS

Samples were prepared from $Ca(NO_3)_2 \cdot 4H_2O$ (Johnson Mathey "puratronic" 99.995%) dehydrated by heating to ~200 °C for several hours, to which the appropriate amount of KNO_3 (Aldrich Chemical 99.999%) was then added to produce the 40–60 mol % CKN mixture, $0.4Ca(NO_3)_2$-$0.6KNO_3$. After removal of surface contamination, the liquid samples were tranferred by pipette to 1.5-cm-diam glass tubes and were degassed by heating for 12–24 h in an oven at ~300 °C. The samples were then removed from the oven and sealed with Teflon tape. They were clear with very few visible air bubbles or dust particles. No crystallization was observed even after long periods at 130 °C, where rapid crystallization was reported previously,[33] or after slow cooling to room temperature or lower.

The sample tube was mounted in a custom-made high temperature optical access oven. The oven's thermocouple was calibrated by installing a sample tube containing paraffin oil and inserting a calibrated thermistor in the oil. (The measured 5-K difference was subtracted from the thermocouple temperature readings.)

Brillouin spectra were obtained with a Sandercock six-pass tandem Fabry-Pérot interferometer. The optical layout and interferometer performance have been described in detail previously.[34] The incident light was the single-mode 4880-Å line from a Spectra Physics model 165 argon-ion laser with power at the sample of typically 70 mW. Spectra were recorded in a 1024-channel multiscaler, and typically consisted of 2000 scans of $\frac{1}{2}$ sec each.

Polarized (VV) Brillouin spectra at six temperatures are shown by the dots in Fig. 1. At $T = 598$ K (the top spectrum in Fig. 1) the spectrum exhibits two symmetrically placed Brillouin components and an unresolved Rayleigh line consisting of quasielastic scattering from concentration and entropy fluctuations as well as parasitic elastic scattering. As the sample is cooled (from top to bottom in Fig. 1), the frequency shift of the Brillouin peaks increases, while the Brillouin linewidth increases, reaches a maximum at ~485 K, and then decreases. Associated with the changes observed in the Brillouin peaks, an additional central component appears and narrows continuously as the temperature decreases, finally disappearing into the unresolved Rayleigh line.

The depolarized (VH) Brillouin spectra at $\theta = 90°$ are shown in Fig. 2 (538–478 K) and in Fig. 3 (438–328 K). In Fig. 2, a central mode is clearly seen, which narrows as the temperature decreases. This feature was also observed by Grimsditch and co-workers[35,36] who attributed it to orientational dynamics of the NO_3^- ions. This assignment is consistent with our observations that its width is identical in $\theta = 90°$ and 180° spectra, and that its intensity does not vanish at $\theta = 180°$ so that it cannot be due to the overdamped TA mode for which $I_{TA} \propto \cos^2(\theta/2)$.

At temperatures below ~423 K, as shown in Fig. 3, the depolarized spectra exhibit resolvable Brillouin peaks,

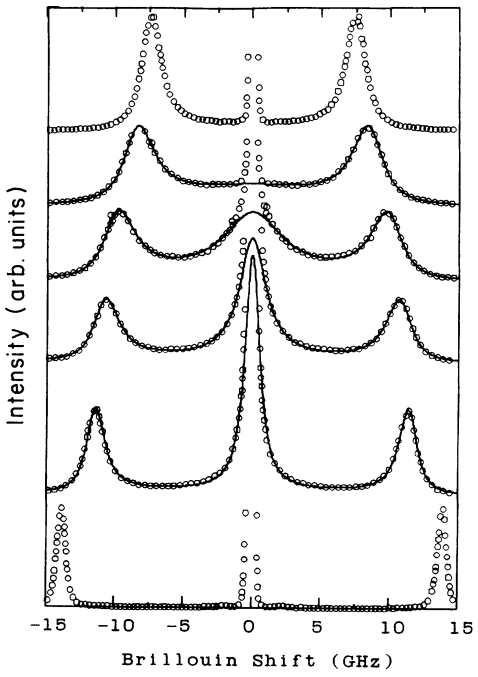

FIG. 1. Experimental polarized CKN 90° Brillouin spectra at (top to bottom) 598, 528, 478, 448, 428, and 348 K. The circles are the experimental data. Solid lines are the results of fits of the middle four spectra to Eq. (19) with the parameters given in Table I. (The vertical scales of successive spectra have been shifted arbitrarily to improve visibility.)

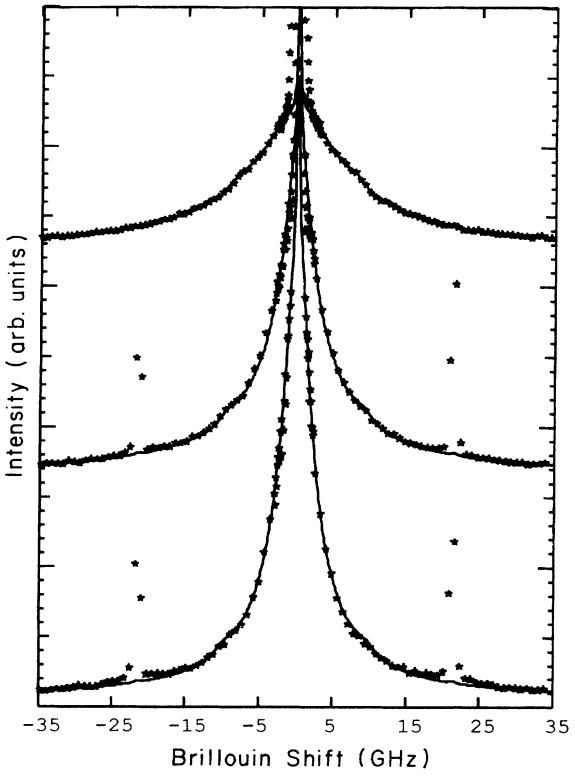

FIG. 2. Depolarized (VH) high-temperature 90° Brillouin spectra of CKN at (top to bottom) 538, 498, and 478 K. Solid lines are fits to Eq. (21) with the parameters given in Table II. (For clarity, only $\frac{1}{8}$ of the data points are shown. The extra features near 22 GHz are ghosts of the Rayleigh line).

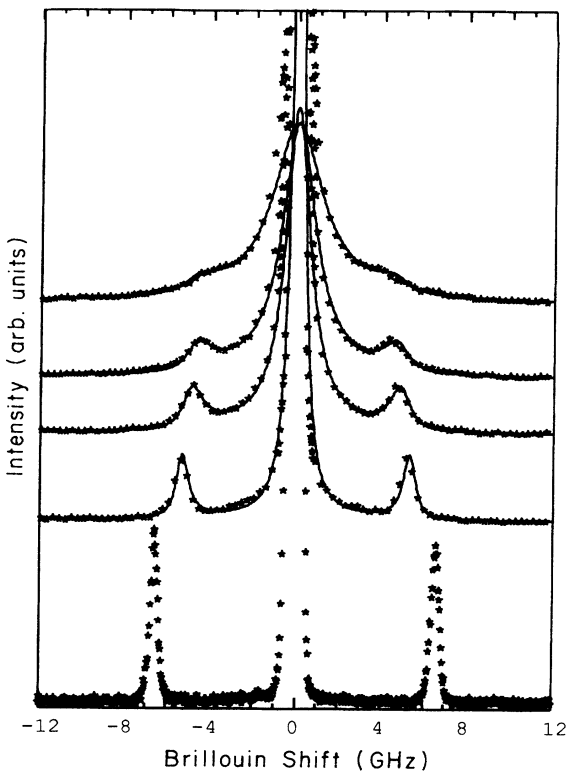

FIG. 3. Depolarized (VH) 90° Brillouin spectra of CKN at (top to bottom) 438, 418, 408, 388, and 328 K showing the emergence of the transverse-acoustic modes. Solid lines are fits to the upper four spectra using the phenomenological model of Eqs. (22) and (23) with the parameters given in Table III.

which sharpen and move towards higher frequency with decreasing temperature. We note that these TA modes were not observed in the $\theta=180°$ spectra, as predicted by the $I_{TA} \propto \cos^2(\theta/2)$ result.

IV. ANALYSIS OF POLARIZED BRILLOUIN SPECTRA

A set of 12 polarized $\theta=90°$ CKN Brillouin spectra at temperatures from 428 to 538 K in 10-K steps, plus one high-temperature (598-K) spectrum and one low-temperature (348-K) spectrum were analyzed numerically. The relevant information for the 12 spectra is shown in Table I. All spectra were collected with the same free spectral range (15.79 GHz), with a frequency scale of 0.0356 GHz/channel.

The theoretical density fluctuation spectrum [$\mathrm{Re}\{\tilde{R}(\omega)\}$ in Eq. (13)] was computed with $\tilde{\Gamma}(q,\omega)$ from Eqs. (14) and (17). For $\phi(q_0,t)$ we used the neutron spin-

TABLE I. Parameters used in fits of polarized (VV) CKN Brillouin spectra [Eq. (19)]. a, β, τ are the stretched exponential $\phi(q_0,t)$ parameters from Ref. 10. Γ_R is the rotational relaxation rate from Lorentzian fits to depolarized spectra. The coupling constant V_{PY} computed from the Percus-Yevick equation with Eq. (18) is shown for comparison with the value resulting from the fit.

	$\phi(k_0,t)$ Mezei			Fit parameters							
T (K)	a	τ (10^{-11} sec)	β	Rot. Γ_R (10^9 rad/sec)	ω_0 (10^9 rad/sec)	h_1 (10^3)	h_2 (10^3)	I_{bg}	$(V_0)^{1/2}$ (10^9 rad/sec)	$(V_{PY})^{1/2}$ (10^9 rad/sec)	χ_R^2
538	0.84	0.97	0.58	42.9	49.2	8.6	0.20	17	66.0	16.4	1.27
528	0.84	1.15	0.58	36.2	50.1	7.7	0.17	23	65.1	16.8	1.12
518	0.84	1.40	0.58	34.2	50.3	7.7	0.26	17	62.7	16.9	1.40
508	0.84	1.70	0.58	30.4	51.4	9.4	0.36	17	62.9	17.3	1.53
498	0.84	2.15	0.58	24.1	52.1	8.8	0.43	26	61.0	17.5	1.49
488	0.84	2.80	0.58	19.5	52.9	8.7	0.56	28	59.5	17.9	1.49
478	0.84	3.70	0.58	15.0	53.8	7.9	0.66	31	58.1	18.2	1.62
468	0.84	5.20	0.58	12.4	54.9	6.4	0.67	28	56.9	18.6	1.58
458	0.84	7.60	0.58	10.3	54.2	7.8	0.88	37	55.9	18.4	1.63
448	0.84	11.50	0.58	6.60	54.5	7.2	1.1	36	58.4	18.5	1.34
438	0.84	19.50	0.58	4.81	54.2	8.4	1.6	47	57.5	19.1	2.06
428	0.84	36.50	0.58	3.80	54.4	8.2	1.3	46	60.8	18.9	2.06

echo results of Mezei, Knaak, and Farago[10] who found that in this temperature range $\phi(q_0,t)$ can be accurately represented by a stretched exponential[37] with $\beta=0.58$, $A=0.84$, and $\tau(T)=6\pi\eta R/k_BTq_0^2$, where $R=0.75$ Å, $q_0=1.7$ Å^{-1}, and $\eta(T)$ was taken from the viscosity measurements of Glover and Matheson.[38] To complete the calculation of $\tilde{\Gamma}(q,\omega)$, $\phi^2(q_0,t)$ was Fourier transformed numerically with a fast-Fourier-transform Port Library program, the coupling constant V_0 was treated as an adjustable parameter, and $\Gamma_0=2.24\times10^9$ rad/sec was determined from the low-temperature (348-K) Brillouin spectrum and assumed to be temperature independent.

An extra complication arises in CKN from the fact that rotational motion of the NO_3^- ions contributes to both depolarized and polarized spectra. (We will discuss the rotational problem in detail in the following section.) In the frequency range of our polarized spectra (±15 GHz), analysis of depolarized spectra shows that the rotational scattering can be accurately fit by a Lorentzian function $(\omega^2+\Gamma_R^2)^{-1}$, where Γ_R is a rotational relaxation rate. To determine the values Γ_R, we therefore accumulated a depolarized spectrum at each of the temperatures in Table I and performed a Lorentzian fit.

The total theoretical function to which the spectra were fitted was therefore

$$I(\omega)=h_1\frac{\omega_0^2\Gamma'\Gamma_0}{[\omega^2-(\omega_0^2+\omega\Gamma'')]^2+(\omega\Gamma')^2}+h_2\frac{\Gamma_R^2}{(\omega^2+\Gamma_R^2)}+I_{\rm bg}\ , \tag{19}$$

where

$$\Gamma(\omega)=\Gamma'+i\Gamma''=\Gamma_0+V_0\int_0^\infty e^{i\omega t}[Ae^{-(t/\tau)^\beta}]^2dt\ .$$

In Eq. (19), h_1 and h_2 are the (dimensionless) amplitudes of the density fluctuation and rotational parts of the spectrum and $I_{\rm bg}$ is a frequency-independent background. The dimensionless functions, which h_1 and h_2 multiply have been chosen so that h_2 is the intensity of the rotational part at $\omega=0$ and h_1 is (approximately) the intensity of the density fluctuation part at the Brillouin peak.

In Eq. (19), the five free parameters h_1, h_2, $I_{\rm bg}$, ω_0, and V_0 were optimized using the Port Library NLLSQ nonlinear least-squares fitting program. Fits were carried out in the range ±1–15 GHz to avoid the interferometer ghosts near ±16 GHz and the Rayleigh line. In the fits, the theoretical spectra of Eq. (19) were convoluted with the instrumental response taken from the experimentally observed Rayleigh line. The optimum values of the parameters and the resulting reduced χ_R^2 values are given in Table I. Note that if we had used a phenomenological fitting function such as Eq. (11) or (12), there would have been seven free parameters instead of five.

The coupling constant V_0 of Eq. (17) was treated as a free parameter in the fits. However, we also computed V_0 from Eq. (18), using the Percus-Yevick equation to calculate $S(q_0)$ as discussed in Ref. 19. The resulting values are listed in Table I as $V_{\rm PY}$. These values agree with the results of the fits to within a factor of 4, which is very good in view of the inadequacy of the hard-sphere approximation of the Percus-Yevick equation for molten salts.

V. DEPOLARIZED BRILLOUIN SPECTRA

In analyzing the depolarized Brillouin spectra, two effects of the optical anisotropy of the NO_3^- ions must be considered. First, orientational dynamics due to rotational diffusion cause light scattering directly. Second, because the shape of the ion is also anisotropic, its rotational motion can couple to the local shear flow producing a complicated spectral profile connected with the transverse acoustic modes. We consider these two aspects of the orientational dynamics separately in this section. A comprehensive discussion of light scattering from orientational processes can be found in the book of Berne and Pecora.[39]

A. Light scattering from orientational relaxation

NO_3^- is a planar ion with a threefold axis perpendicular to the molecular plane. Rotations about axes perpendicular to the threefold rotation axis cause polarizability fluctuations and give rise to a depolarized scattered spectrum with intensity $\propto(\alpha_\perp-\alpha_\parallel)^2$, where $\alpha_\perp$ and $\alpha_\parallel$ are the ionic polarizabilities perpendicular and parallel to the plane.

In dilute solutions, the orientational diffusion of noninteracting anisotropic molecules leads to a correlation function for polarizability fluctuations $C(t)\propto e^{-t/\tau_R}$ where $\tau_R=1/6D_R$ and D_R is the rotational diffusion constant. The resulting spectrum is a Lorentzian:

$$I_{VH}=I_0\frac{1}{1+\omega^2\tau_R^2}\ . \tag{20}$$

In concentrated solutions such as the glass forming materials, the single relaxation-time approximation is inadequate, and is frequently replaced by a stretched exponential so that

$$I_{VH}=I_0\,{\rm Re}\left[\int_0^\infty e^{-(t/\tau_R)^\beta}e^{i\omega t}dt\right]\ . \tag{21}$$

An early experimental determination of τ_R for CKN was reported in 1972 by Clarke and Miller.[40] Since the Raman linewidth of a totally symmetric vibrational mode is modified by molecular rotation for depolarized scattering only, they measured the linewidths of the polarized and depolarized ν_1 Raman line of NO_3^- at 1050 cm^{-1}. At a temperature ~200 K above T_g, the depolarized halfwidth [full width at half maximum (FWHM)] exceeded the polarized halfwidth by ~2.4 cm^{-1}, implying a rotational relaxation time τ_R of roughly 4.5×10^{-12} sec. The difference in linewidths decreased with decreasing temperature, vanishing at T_g, indicating an arrest of NO_3^- orientational motion in the glass state. Grimsditch and Torell[36] reported depolarized Brillouin scattering experiments from which they determined $\tau_R\sim2.7\times10^{-11}$ sec at 460 K.

Recently, Signorini, Barrat, and Klein[41] carried out

molecular dynamics calculations on CKN, which included an analysis of orientational relaxation. One interesting result of their analysis was that at 350 K reorientation occurs almost exclusively through large orientational jumps signaling the dominant role of activated hopping processes in the supercooled melt close to T_g. For the polarization relaxation function $C_2(t)$, they found that the slow α-relaxation function could be fit by a stretched exponential function $C_2(t)=0.76e^{-(t/\tau)^{\beta}}$ with $\beta=0.42$. The corresponding relaxation time τ_R was found to increase from $\sim 2.5\times10^{-9}$ sec at $T=700$ K to 2.5×10^{-7} sec at $T=350$ K.

Our depolarized Brillouin spectra at temperatures above 475 K, where no transverse Brillouin components occur, were analyzed as pure rotational scattering. The interferometer's free spectral range was adjusted for each spectrum to provide optimum resolution and signal-to-noise ratios. Lorentzian fits were found to work quite well, but the fit was improved, especially in the wings, by using the stretched exponential form, Eq. (21). The resulting $\beta=0.70\pm0.02$ was essentially temperature independent. The fits to the three spectra ($T=478$, 498, and 538 K) are shown by the solid lines in Fig. 2. Because the polarized spectra are much more intense than the depolarized spectra, a small leakage of the VV spectra through the imperfect polarizer was superimposed on the VH spectra and was included in the fitting procedure. All fitting parameters are listed in Table II. (Note that for each T there are two spectra with different free spectral ranges.) In Fig. 4 we show the values of τ_R found from our analysis along with two values of Grimsditch and Torell,[36] three values deduced from the Raman results of Clarke and Miller,[40] and the molecular dynamics results of Signorini, Barrat, and Klein.[41] The agreement is seen to be good, supporting the interpretation by Grimsditch and Torell of the depolarized central component as being due to rotational diffusion of NO_3^- ions.

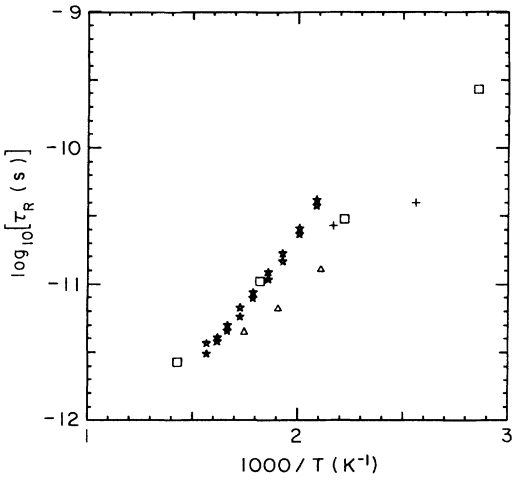

FIG. 4. Arrhenius plots of the rotational relaxation time τ_R vs $1000/T$ from fits to our high-temperature depolarized spectra (*) shown in Table II. The molecular dynamics results of Signorini, Barrat, and Klein (Ref. 41) are shown by (□). Two values determined in a previous Brillouin scattering experiment by Grimsditch and Torell (Ref. 36) are indicated by (+). Three approximate values estimated from the Raman scattering experiment of Clarke and Miller (Ref. 40) are shown by (Δ).

The Arrhenius plot of our rotational relaxation times shown in Fig. 4 can be fit by a straight line, which shows that, at least in this limited temperature range, a simple Arrhenius law for τ_R applies. The slope of the linear fit gave an activation energy of 8.5 Kcal/mol.

TABLE II. Parameters used in fits of depolarized (VH) Brillouin spectra ($T\geq 478$ K) [Eq. (21)]. Leakage represents the (small) additional intensity contributed by the polarized spectrum due to imperfect polarizers and I_{bg} is a constant background. Note that for each T there are two spectra with different free spectral ranges.

T (K)	GHz (per ch.)	$1/\tau_R$ (ch.)	τ_R (10^{-12} sec)	β	I_{bg}	I_0	Leakage	χ_R^2
638	0.2232	1224	3.7	0.71	26	746	5×10^{-3}	1.1
638	0.4464	737	3.1	0.71	20	645	4×10^{-3}	1.0
618	0.2232	1099	4.1	0.72	21	697	3×10^{-3}	1.0
618	0.3348	799	3.8	0.72	22	653	4×10^{-3}	0.9
598	0.2232	890	5.0	0.70	21	745	3×10^{-3}	1.1
598	0.3348	651	4.6	0.70	25	880	2×10^{-3}	0.9
578	0.2678	656	5.7	0.67	20	699	4×10^{-3}	1.2
578	0.1339	1095	6.8	0.70	20	873	4×10^{-3}	1.1
558	0.1339	858	8.7	0.72	24	959	7×10^{-3}	1.0
558	0.2678	470	7.9	0.73	30	857	9×10^{-3}	1.4
538	0.0837	969	12.3	0.72	39	1307	17×10^{-3}	0.8
538	0.1674	548	10.9	0.68	26	1146	6×10^{-3}	1.5
518	0.0837	710	16.8	0.73	41	1733	4×10^{-3}	0.9
518	0.1674	407	14.7	0.72	37	1638	7×10^{-3}	1.1
498	0.0478	813	25.7	0.71	30	1527	14×10^{-3}	0.9
498	0.0957	450	23.2	0.69	31	1464	13×10^{-3}	1.0
478	0.0957	272	38.4	0.72	17	1041	2×10^{-3}	1.2
478	0.0478	507	41.4	0.72	23	1310	7×10^{-3}	1.3

B. Transverse-acoustic modes

In a fluid consisting of optically isotropic molecules, transverse velocity does not couple to the optical properties, so the viscous shear modes do not contribute to the light-scattering spectrum. In fluids containing large optically and mechanically anisotropic molecules, transverse velocity couples to molecular orientations and therefore can produce light scattering.

Fabelinskii and co-workers[42] and Stoicheff and co-workers[43,44] discovered that the low-frequency depolarized spectra of several molecular fluids (such as quinoline) exhibit a novel central peak with a narrow central dip producing a minimum at the center. Initially interpreted as evidence for propagating shear waves, this unusual spectral shape was subsequently shown to result from a subtle interference between direct scattering due to rotational diffusion and scattering from orientational fluctuations produced by coupling of molecular orientation to the local shear stress.[31,39,45]

Wang[46] and Wang and Zhang[47] proposed an extension of the orientation-shear stress coupling model that includes the viscoelastic properties of the undercooled liquid to explain the temperature dependence of depolarized Brillouin spectra near the glass transition. We attempted to fit our data to the theory of Wang and Zhang with limited success. Although the theory fit our data quite well at some temperatures, it did not fit the data throughout the full temperature range studied.

An essential difference between ordinary liquids and solids is that transverse modes in high-temperature fluids produce light scattering only if the liquid contains anisotropic molecules, while solids, even if composed of completely isotropic constituents, can exhibit depolarized scattering from transverse-acoustic modes. In the solid, the coupling occurs through the distortion of electronic wave functions by shear strains expressed as the transverse Pockel's coefficient (or photoelastic constant) p_{44}. As shown in our paper on LiCl-H_2O,[19] the appearance of TA modes in undercooled liquids approaching the liquid-glass transition can be described by $I_{VH}(\omega) \propto p(\omega) J_T(\omega)/\omega^2$, where $J_T(\omega)$ is the transverse velocity correlation function,[31] and the photoelastic constant $p(\omega)$ is assumed to be frequency dependent with the same relaxation time τ_S as the shear viscosity, as originally proposed by Rytov.[48] The resulting phenomenological expression for $I_{VH}(\omega)$ is

$$I_{VH}(\omega)=I_0\frac{p(\omega)K_0\tau_S^2/(1+\omega^2\tau_S^2)}{[\omega^2-q^2K_0\omega^2\tau_S^2/(1+\omega^2\tau_S^2)]^2+[\omega q^2K_0\tau_S/(1+\omega^2\tau_S^2)]^2} \tag{22}$$

with

$$p(\omega)=\omega^2\tau_S^2/(1+\omega^2\tau_S^2)\ . \tag{23}$$

In Eq. (22), K_0 is the square of the shear-mode velocity in the high-frequency limit $\omega\rightarrow\infty$.

Depolarized 90° Brillouin scattering spectra in the temperature range 438 K $>T>$ 388 K were analyzed starting from Eq. (22), with the contribution to the spectrum due to rotational diffusion [Eq. (21)] added, with $\beta=0.7$. The estimated rotational relaxation times τ_R shown in Table III were obtained from an Arrhenius fit to the high-temperature *VH* results shown in Table II, which gave $\tau_R=0.001\,89e^{-4712/T}\times10^{-12}$ sec. The amplitudes of the transverse velocity and rotational diffusion contributions, I_0 and h_2, along with resulting values of τ_S, $qK_0^{1/2}$ and the background (I_{bg}) given by the fits are shown in Table III. The quality of the fits was excellent, as can be seen in Fig. 3.

VI. PREVIOUS EXPERIMENTS

CKN has been the subject of many previous experiments. The temperature dependence of its shear viscosity $\eta_s(T)$ was studied by Rhodes, Smith, and Ubbelohde,[49] Glover and Matheson,[38] and Tweer, Laberge, and Macedo.[50] Glover and Matheson found that for $T>390$ K, η_s can be accurately represented by

$$\log_{10}\eta_s=-3.1512+\frac{277.32\ \text{K}}{T-382.97\ \text{K}} \tag{24}$$

[with η_s in Ns/m^2, where 1 Ns/m^2=10 P; note that Eq. (24) was used in computing the relaxation times listed in Table I]. Tweer, Laberge, and Macedo[50] showed that although an Arrhenius plot of $\log_{10}\eta_s$ versus $1/T$ falls on a smooth curve spanning the range $0\le\log_{10}\eta_s\le14$, a single Vogel-Tamman-Fulcher expression $\eta_s=A\exp[C/(T-T_0)]$ such as Eq. (24) cannot provide an acceptable fit over the whole range.

TABLE III. Parameters used in fits of depolarized (*VH*) spectra ($T\le438$ K) [Eq. (22)] h_2 scales the additional contribution due to orientational motion of the NO_3^- ions.

T (k)	I_0	τ_s (10^{-11} sec)	τ_R (10^{-11} sec)	$K_0^{1/2}q$ (10^9 rad/sec)	I_{bg}	h_2	χ_R^2
438	2762	10.2	8.9	4.35	37	1.6	1.7
418	3776	15.6	14.8	4.39	38	1.2	1.5
408	8958	21.2	19.5	4.56	76	1.8	1.6
398	6855	27.1	26.1	4.77	57	0.9	1.5
388	2686	53.2	35.4	4.93	25	0.6	1.5

The electrical conductivity and dielectric response of CKN were also studied by Rhodes, Smith, and Ubbelohde,[49] and by Howell *et al.*[51] who found that the width of the peak in the imaginary part of the dielectric contant ϵ'' becomes *broader* with increasing temperature, implying an apparent decrease in the stretching parameter β. This behavior was ascribed to a change in the conductivity mechanism with increasing temperature, involving the effects of microscopic heterogeneity on the hopping rate.[51]

Weiler, Bose, and Macedo[52] performed ultrasonic experiments on CKN in the temperature range $363 \leq T \leq 402$ K. In these experiments, the width of the distribution of relaxation times $g(\tau_L)$ was again found to be temperature dependent, decreasing markedly at high temperatures. This behavior is consistent with several other observations (as we will discuss in the next section).

Two inelastic neutron-scattering studies of CKN by Mezei and co-workers[10,11] provided critical insights into the dynamics of the short-wavelength structural dynamics near the glass transition. Their neutron spin-echo experiments[10] revealed that $\phi(q_0,t)$ decays with two components as predicted by MCT, the slower of which has the stretched exponential form and shows critical slowing down with decreasing temperature. They also verified the scaling-law prediction of MCT by replotting the data on a master plot [$\phi(t/\tau)$ versus t/τ]. However, recent data covering an extended time domain suggest that the scaling result may only be approximately valid.[53] In a subsequent neutron-scattering study that combined time-of-flight and spin-echo data, Knaak, Mezei, and Farago[11] showed that the scattering functions $S(q_0,\omega)$ display two power-law regimes with a temperature-dependent crossover frequency as predicted by MCT.

Light-scattering spectroscopy has been widely employed to study CKN. The Raman scattering experiments of Clarke and Miller[40] provided the first estimate of the NO_3^- rotational relaxation time, as discussed in Sec. V and shown in Fig. 4. Sidebottom and Sorensen[23] performed depolarized photon correlation measurements on CKN, and fit their data to a stretched exponential. In the range 341 K $< T <$ 358 K they found a constant $\beta \sim 0.40$ and a rotational relaxation time, which increased from 2.8×10^{-3} sec at 359 K to 150 sec at 341 K. Cheng, Yan, and Nelson[25] exploited the newly developed time-resolved technique of impulsive stimulated Brillouin scattering to probe the acoustic properties of CKN. Their experiment also showed that the acoustic damping, plotted against $\log_{10}(\omega)$, exhibits a peak that narrows with increasing temperature, consistent with the ultrasonic result of Weiler, Bose, and Macedo.[52]

Brillouin scattering studies of CKN have been reported previously by Torell,[33] Torell and Aronsson,[54] Grimsditch, Bhadra, and Torell,[35] and Grimsditch and Torell.[36] In these studies, the Brillouin shifts and linewidths were measured for the longitudinal and transverse modes, but no attempt was made to fit the overall spectra to specific theoretical models. In the paper by Torell and Aronsson, the temperature dependence of the high-frequency sound velocities $v_{L,\infty}$ and $v_{T,\infty}$ deduced from their data are shown and exhibit a sharp change of slope at T_g. As we have previously noted,[19] similar changes in slope have been observed in a number of Brillouin scattering studies on other materials as well.[55] The fact that the temperature dependence of the sound velocity determined by ultrasonic measurements changes at the glass transition was also noted in the book by Hertzfeld and Litovitz.[56]

The experiments of Grimsditch and Torell[36] and Grimsditch, Bhadra, and Torell,[35] demonstrated that at high temperatures the depolarized spectrum is primarily due to NO_3^- orientational dynamics, a point that we have further explored in Sec. V, and shown to be in good agreement with the molecular dynamics results of Signorini, Barrat, and Klein[41] (see Fig. 4).

Finally, in a recent depolarized Brillouin scattering study of CKN,[14] we have shown that the spectrum, when measured over several decades in frequency, exhibits self-similarity and two regions of power-law behavior resembling the neutron-scattering results of Knaak, Mezei, and Farago.[11] Recently, we have concluded that the mechanism responsible for this extended depolarized spectrum is second-order scattering from two modes at $\pm q_0$.[57] It is therefore possible to compare directly the broad-band depolarized light-scattering spectrum with neutron-scattering data or with numerical predictions of MCT, as we shall show in a forthcoming publication.[58]

VII. DISCUSSION AND CONCLUSIONS

We have shown that the polarized Brillouin spectra of CKN can be accurately described by the MCT in the approximation that the long-wavelength acoustic mode is damped by anharmonic coupling to pairs of density fluctuation modes at q_0. In our analysis, the density correlation function of the q_0 modes was taken from the neutron spin-echo experiments of Mezei, Knaak, and Farago.[10] The excellent fits obtained provide strong support for the correctness of the physical mechanism underlying the MCT. However, it does *not* demonstrate either the form of the memory function or the validity of the time-temperature superposition principle (scaling). The Brillouin experiments span a temperature range in which the viscosity only increases from ~ 0.1 to ~ 5 P and a frequency range of 1 to 15 GHz, which is not a very large dynamic range. As recently emphasized by Fuchs, Götze, and Latz,[16] it is not possible to reliably determine if scaling holds with a limited dynamic range. In fact, we have tried fitting both real and simulated Brillouin data with the stretched exponential function [Eq. (11)] or the Cole-Davidson function [Eq. (12)], and have found that it is extremely difficult to determine β accurately unless the accessible spectral region extends well below 1 GHz and the spectra can be accumulated for long enough times so that the Poisson noise is well below the 1% level. We also reanalyzed the neutron data[10] with $\beta = 1$, assuming that scaling applies. The resulting master plot was clearly inferior to the plot with $\beta = 0.58$. Nevertheless, the resulting A and τ values, when inserted in the expression for $\Gamma(\omega)$ in Eq. (19), led to fits to the Brillouin data that were not noticeably different from the $\beta = 0.58$ fits shown in Fig. 1, although χ_R^2 increased by $\sim 15\%$. We therefore

conclude that it is generally very difficult to determine β reliably in Brillouin scattering experiments unless ω_0 can be determined independently by ultrasonic measurements.

There are, however, a number of other experiments which suggest that scaling may be only approximately valid. If a relaxation function is written as

$$\phi(t)=\int_0^\infty g(\tau)e^{-(t/\tau)}d\tau\ , \tag{25}$$

where $g(\tau)$ represents the distribution of relaxation times, then in the single relaxation time limit $g(\tau)=\delta(\tau-\tau_0)$, the imaginary part of the corresponding susceptibility $\chi''\propto\omega\tau_0/[1+(\omega\tau_0)^2]$ plotted against $\log_{10}(\omega)$ is symmetric with a full width of 1.14 decades.[2,51] Any increase in the width of the distribution function $g(\tau)$ leads to an increase in width. If $\phi(\tau)$ is parametrized as the stretched exponential function, Eq. (11), then any value of $\beta<1$ produces a width >1.14 decades in the χ'' versus $\log_{10}(\omega)$ plot. Thus a temperature-dependent width implies that β is also temperature dependent, which would violate scaling.

The recent dielectric susceptibility study of salol by Dixon *et al.*[59] clearly exhibit a broadening and loss of symmetry in the ϵ'' versus $\log_{10}(\omega)$ plots with decreasing temperature. Similarly, the acoustic damping in CKN determined by Cheng, Yan, and Nelson[25] (see their Fig. 5), also exhibits marked broadening with decreasing temperature.[60] Angell and Torell[61] have reviewed much of the experimental evidence for increase of the width of absorption peaks with decreasing temperature, and have demonstrated such an effect in CKN by combining the Brillouin data of Torell[33] with the ultrasonic data of Weiler, Bose, and Macedo,[52] although Fuchs, Götze, and Latz[16] have challenged this analysis. We have also reanalyzed an extended set of CKN neutron spin-echo data of Mezei and co-workers[10,53] and found that, while a good scaling fit (or "master plot") can be achieved with $\beta\sim0.58$, individual fits of the data at each temperature to stretched exponentials gave improved fits with β allowed to vary, and the results of the fits indicate a tendency for β to increase with temperature from ~0.52 at 403 K to ~0.71 at 553 K. Mezei[53] has also reanalyzed the extended neutron data and has also found a temperature-dependent value for β. We note, however, that this result (absorption width decreasing with increasing temperature) is not universal. In some experiments the width of the χ'' curve apparently increases with increasing temperature rather than decreasing.[62]

Fuchs, Götze, and Latz[16] have reviewed much of the Brillouin and ultrasonic data for CKN and argued that it is possible to present all of it on a single master plot, indicating that scaling is valid and that the stretching parameter β is therefore independent of temperatures, with a value of 0.44. We would suggest, however, that their procedure only demonstrates that scaling is approximately valid. A more stringent test requires separately analyzing data at each temperature to see if significant improvements in χ^2 (or some other goodness of fit criterion) can be achieved with a temperature-dependent β.

We believe, however, that it is probably not possible to definitely establish the validity of scaling from the analysis of experimental data, except within some limited temperature range. At temperatures close to T_g, the dominance of activated hopping processes will modify the structural dynamics, while at high temperatures, as recently noted by Mezei,[53] the time scales of the α and β relaxation processes become similar, making it more difficult to exclude the contributions of β relaxation from the fitting procedure.

Extensions of the mode-coupling theory beyond the asymptotic regime $T\rightarrow T_c^+$, where scaling is expected to hold, are currently under development, however, and further attempts to test the predictions of the extended MCT present an exciting challenge for the future.

ACKNOWLEDGMENTS

We wish to thank W. Götze, C. A. Angell, L. M. Torell, R. Pick, and M. C. Marchetti for helpful suggestions, and especially F. Mezei for generously providing numerical neutron spin-echo data from experiments performed since those reported in Refs. 10 and 53 for use in this study. This research was supported by the National Science Foundation under Grant Nos. DMR-8614168 and DMR-9014344, and, in part, by the Science Division of the City College of New York.

*Present address: Department of Physics, Arizona State University, Tempe, AZ 85287.

[1]G. H. Fredrickson, Ann. Rev. Phys. Chem. **39**, 149 (1988).

[2]J. Jackle, Rep. Prog. Phys. **49**, 171 (1986).

[3]C. A. Angell, J. Non-Cryst. Solids **73**, 1 (1985).

[4]A comprehensive overview of much of the recent work in this field appears in *Dynamics of Disordered Materials*, edited by D. Richter, A. J. Dianoux, W. Petry, and J. Teixeira (Springer-Verlag, Berlin, 1989).

[5]U. Bengtzelius, W. Götze, and A. Sjolander, J. Phys. C **17**, 5915 (1984).

[6]E. Leutheusser, Phys. Rev. A **29**, 2765 (1984).

[7]For a recent comprehensive review of MCT see W. Götze, in *Liquids, Freezing and the Glass Transition, Les Houches, 1989*, edited by J. P. Hansen, D. Levesque, and J. Zinn-Justin (North-Holland, Amsterdam, 1990).

[8]C. A. Angell, J. Phys. Chem. Solids **49**, 863 (1988).

[9]W. Götze and L. Sjögren, Z. Phys. B **65**, 415 (1987).

[10]F. Mezei, W. Knaak, and B. Farago, Phys. Rev. Lett. **58**, 571 (1987).

[11]W. Knaak, F. Mezei, and B. Farago, Europhys. Lett. **7**, 529 (1988).

[12]D. Richter, B. Frick, and B. Farago, Phys. Rev. Lett. **61**, 2465 (1988).

[13]B. Frick, B. Farago, and D. Richter, Phys. Rev. Lett. **64**, 2921 (1990).

[14]N. J. Tao, G. Li, and H. Z. Cummins, Phys. Rev. Lett. **66**, 1334 (1991).

[15]I. A. Campbell, J.-M. Flesselles, R. Jullien, and R. Botet, Phys. Rev. B **37**, 3825 (1988).
[16]M. Fuchs, W. Götze, and A. Latz, Chem. Phys. **149**, 185 (1990).
[17]M. Soltwisch, J. Sukmanowski, and D. Quitmann, J. Chem. Phys. **86**, 3207 (1987).
[18]L. Börjesson, M. Elmroth, and L. M. Torell, Chem. Phys. **149**, 209 (1990).
[19]N. J. Tao, G. Li, and H. Z. Cummins, Phys. Rev. B **43**, 5815 (1991).
[20]C. A. Angell, in *Correlations and Connectivity,* edited by H. E. Stanley and N. Ostrowsky (Kluwer Academic, New York, 1990), p. 133.
[21]R. D. Mountain, Revs. Mod. Phys. **38**, 205 (1966); J. Res. Nat. Bur. Stand. **70A**, 207 (1966); **72A**, 95 (1968).
[22]C. Demoulin, C. J. Montrose, and N. Ostrowsky, Phys. Rev. A **9**, 1740 (1974); C. Allain and P. Lallemand, J. Phys. (Paris) **40**, 693 (1979).
[23]D. L. Sidebottom and C. M. Sorensen, J. Chem. Phys. **91**, 7153 (1989).
[24]C. Allain, M. Berard, and P. Lallemand, Mol. Phys. **41**, 429 (1980).
[25]L. T. Cheng, Y. X. Yan, and K. A. Nelson, J. Chem. Phys. **91**, 6052 (1989).
[26]C. J. Montrose, V. A. Solovyev, and T. A. Litovitz, J. Acoust. Soc. Am. **43**, 117 (1968).
[27]In Eq. (10), ω_0 is the acoustic frequency in the low-frequency limit, $\omega\tau \ll 1$. In Ref. 19 we used an equivalent equation containing ω_∞, the high-frequency limiting value for $\omega\tau \gg 1$. The two are related by $\omega_\infty^2 = \omega_0^2 + \Delta^2$.
[28]J. D. Axe, S. M. Shapiro, G. Shirane, and T. Riste, in *Anharmonic Lattices, Structural Transitions and Melting,* edited by T. Riste (Noordhoff, Leiden, 1974), p. 23. (Several excellent discussions of the central-peak problem can be found in this volume.)
[29]P. Bezot, C. Hesse-Bezot, J. P. Petitet, and D. Roynard, J. Mol. Liq. **34**, 317 (1987).
[30]C. P. Lindsey and G. D. Patterson, J. Chem. Phys. **73**, 3348 (1980).
[31]J. P. Boon and S. Yip, *Molecular Hydrodynamics* (McGraw-Hill, New York, 1980).
[32]T. R. Kirkpatrick, Phys. Rev. A **31**, 939 (1985).
[33]L. M. Torell, J. Chem. Phys. **76**, 3467 (1982).
[34]G. Li, N. J. Tao, Le Van Hong, H. Z. Cummins, C. Dreyfus, M. Hebbache, R. M. Pick, and J. Vagner, Phys. Rev. B **42**, 4406 (1990).
[35]M. Grimsditch, R. Bhadra, and L. M. Torell, Phys. Rev. Lett. **62**, 2616 (1989).
[36]M. Grimsditch and L. M. Torell, in *Dynamics of Disordered Materials,* edited by D. Richter, A. J. Dianoux, W. Petry, and T. Teixeira (Springer-Verlag, Berlin, 1989), p. 196.
[37]We also analyzed more recent CKN neutron-spin echo data provided by F. Mezei spanning a larger time range than the data of Ref. 10, and found a similar scaling result with $A = 0.87$, $\beta = 0.60$, and $R = 0.93$ Å. Separate analyses of the data for each temperature indicated a tendency for β to increase somewhat with temperature, a result also seen by Mezei (Ref. 53). Since these parameter changes made only minor changes in the remaining parameters in the fits to our Brillouin data, we carried out our analysis using the parameters of Ref. 10.
[38]G. M. Glover and A. J. Matheson, Trans. Faraday Soc. **67**, 1960 (1971).
[39]B. J. Berne and R. Pecora, *Dynamic Light Scattering* (Wiley, New York, 1976).
[40]J. H.R. Clarke and S. Miller, Chem. Phys. Lett. **13**, 97 (1972).
[41]G. F. Signorini, J. L. Barrat, and M. L. Klein, J. Chem. Phys. **92**, 1294 (1990).
[42]I. L. Fabelinskii and V. S. Starunov, Appl. Opt. **6**, 1793 (1967); V. S. Starunov, E. V. Tiganov and I. L. Fabelinskii, Pis'ma Zh. Eksp. Teor. Fiz. **5**, 317 (1967) [JETP Lett. **5**, 260 (1967)].
[43]G. I. A. Stegeman and B. P. Stoicheff, Phys. Rev. Lett. **21**, 202 (1968); Phys. Rev. A **7**, 1160 (1973).
[44]G. D. Enright and B. P. Stoicheff, J. Chem. Phys. **64**, 3658 (1976).
[45]T. Keyes and D. Kivelson, J. Chem. Phys. **56**, 1876 (1972).
[46]C. H. Wang, Mol. Phys. **58**, 497 (1986).
[47]C. H. Wang and J. Zhang, J. Chem. Phys. **85**, 794 (1986).
[48]S. M. Rytov, Zh. Eksp. Teor. Fiz. **33**, 514 (1957) [Sov. Phys. JETP **6**, 401 (1958)]; **33**, 671 (1957) [**6**, 513 (1958)].
[49]E. Rhodes, W. E. Smith, and A. R. Ubbelohde, Trans. Faraday Soc. **63**, 1943 (1967).
[50]H. Tweer, N. Laberge, and P. B. Macedo, J. Am. Ceram. Soc. **54**, 121 (1971).
[51]F. S. Howell, R.A. Bose, P.B. Macedo, and C. T. Moynihan, J. Phys. Chem. **78**, 639 (1974).
[52]R.Weiler, R. Bose, and P. B. Macedo, J. Chem. Phys. **53**, 1258 (1970).
[53]F. Mezei, J. Non-Cryst. Solids **131**, 317 (1991).
[54]L. M. Torell and R. Aronsson, J. Chem. Phys. **78**, 1121 (1983).
[55]T. Yagi, Physica B **150**, 265 (1988).
[56]K. F. Herzfeld and T. A. Litovitz, *Absorption and Dispersion of Ultrasonic Waves* (Academic, New York, 1959), p. 489.
[57]N. J. Tao, G. Li, X. Chen, W. M. Du, and H. Z. Cummins, Phys. Rev. A **44**, 6621 (1991).
[58]G. Li, W. M. Du, X. Chen, H. Z. Cummins, and N. Tao, Phys. Rev. A (to be published).
[59]P. K. Dixon, L. Wu, S.R. Nagel, B. D. Williams, and J. P. Carini, Phys. Rev. Lett. **65**, 1108 (1990).
[60]For other examples of temperature dependence of the stretching parameter β, see L. M. Torell, L. Börjesson, and M. Elmroth, J. Phys. Condens. Matter **2**, SA207 (1990); and Ref. 52.
[61]C. A. Angell and L. M. Torell, J. Chem. Phys. **78**, 937 (1983).
[62]A. R. Duggal and K. A. Nelson, J. Chem. Phys. (to be published).